


ORIGINAL ARTICLE

Dahuang Fuzi Baijiang decoction restricts progenitor to terminally exhausted T cell differentiation in colorectal cancer

Yihua Xu¹ | Hao Wang¹ | Tao Wang² | Chunhui Chen³ | Ruibo Sun¹ | Wanyu Yao¹ | Ye Ma¹ | Qingyuan Zhang¹ | Liyi Wu¹ | Shanmei Zeng⁴ | Xuegang Sun^{1,5} 

¹The Key Laboratory of Molecular Biology, State Administration of Traditional Chinese Medicine, School of Traditional Chinese Medicine, Southern Medical University, Guangzhou, China

²Department of Urology, Zhongshan Hospital of Traditional Chinese Medicine Affiliated to Guangzhou University of Chinese Medicine, Zhongshan, China

³Department of Gastroenterology, The Second Affiliated Hospital of Guangzhou University of Chinese Medicine, Guangzhou, China

⁴Department of Radiology, The First Affiliated Hospital of Sun Yat-Sen University, Guangzhou, China

⁵Department of Traditional Chinese Medicine, Zhujiang Hospital, Southern Medical University, Guangzhou, China

Correspondence

Xuegang Sun, The Key Laboratory of Molecular Biology, State Administration of Traditional Chinese Medicine, School of Traditional Chinese Medicine, Southern Medical University, Guangzhou, China. 1838, Guangzhou 510515, Guangdong, China.

Email: sgx_smu@126.com

Funding information

Key-Area Research and Development Program of Guangdong Province, Modernization of Chinese medicine in Lingnan, Grant/Award Number: 2020B1111100011; National Natural Science Foundation of China, Grant/Award Number: 81974554, 81774172, 81904075; Planned Science Technology Project of Guangzhou, Grant/Award Number: 202002030111

Abstract

Obesity increases the risk of colorectal cancer (CRC) by 30%. The obese tumor microenvironment compromises antitumor immunity by eliciting exhausted T cells (Tex). Hypothesizing that Dahuang Fuzi Baijiang decoction (DFB) is a combined classical prescription from the "Synopsis of Prescriptions of the Golden Chamber". We first determined that DFB regresses tumor growth in high-fat diet-induced obese mice by expanding the TIM3⁻ subset with intermediate expression of programmed cell death-1 (PD-1^{int}TIM3⁻) and restricting the PD-1^{hi}TIM3⁺ subset. Transcription factor 1 (TCF1) is highly expressed in the PD-1^{int}TIM3⁻ subset but is absent in PD-1^{hi}TIM3⁺ cells. We next confirmed that progenitor PD-1^{int}TCF⁺ cells robustly produce tumor necrosis factor- α (TNF α) and interferon- γ , whereas terminally differentiated PD-1^{int}TCF⁺ cells have defects in generating TNF α . With transgenic *ob/ob* mice, we found that DFB produces cooperative efficacy with anti-PD-1 (α PD-1) by limiting the PD-1^{hi}Tim3⁺ subset and amplifying the PD-1^{int}TCF⁺ population. Finally, we defined the recombinant chemokine C-C-motif receptor 2 (CCR2)⁺CD8⁺ subset as terminal Tex and identified that the differentiation from progenitor to terminal Tex is driven, at least in part, by the chemokine (C-C motif) ligand 2 (CCL2)/CCR2 axis. The CCR2 inhibitor enhances the response to α PD-1 by promoting the counts of progenitor Tex. Altogether, DFB dampens CCL2 and preserves progenitor Tex in the obese microenvironment to restrain CRC progression. These findings provide unambiguous evidence that the

Abbreviations: α PD-1, anti-PD-1; CCL2, chemokine (C-C motif) ligand 2; CCR2, recombinant chemokine C-C-motif receptor 2; CRC, colorectal cancer; DFB, Dahuang Fuzi Baijiang decoction; DIO, diet-induced obese; GdCl₃, gadolinium chloride; HFD, high-fat diet; IFN- γ , interferon- γ ; PD-1, programmed cell death-1; PD-L1, PD-1 ligand; TCF1, transcription factor 1; Tex, terminal exhausted T cell; TGF- β , transforming growth factor- β ; TIL, tumor-infiltrating lymphocyte; TIM3, T-cell immunoglobulin domain and mucin domain 3; TNF- α , tumor necrosis factor- α ; TOX, thymocyte selection-associated high mobility group box.

Yihua Xu, Hao Wang, and Tao Wang contributed equally to this work.

This is an open access article under the terms of the [Creative Commons Attribution-NonCommercial](https://creativecommons.org/licenses/by-nc/4.0/) License, which permits use, distribution and reproduction in any medium, provided the original work is properly cited and is not used for commercial purposes.

© 2022 The Authors. Cancer Science published by John Wiley & Sons Australia, Ltd on behalf of Japanese Cancer Association.

traditional Chinese formula DFB can prevent tumor progression by modulating adaptive immunity and establish a strong rationale for further clinical verification.

KEYWORDS

CCL2, colorectal cancer, Dahuang Fuzi Baijiang decoction (DFB), microenvironment, obesity, T cell exhaustion

1 | INTRODUCTION

Obesity is associated with 55% of diagnosed cancers in women and 24% of diagnosed cancers in men.¹ Each 5 kg/m² gain in body mass index can result in 13%–18% increase of CRC risk.² Obesity contributes to 35.4% of CRC cases in men and 20.8% in women.³ Notably, approximately 40% of all cancer deaths are in large part associated with obesity.¹ Obesity represents a top risk factor and an independent prognostic variable of CRC.

Colorectal cancer is an obesity-related cancer.⁴ Cancer-associated adipocytes secrete various adipokines, growth factors, and sex-steroid hormones, including leptin, CCL2, and insulin-like growth factor-1, to create an immune privileged site. Chemokine (C-C motif) ligand 2 is the pivotal chemokine that orchestrates the formation of an immunosuppressive tumor microenvironment by empowering adipocytes to maintain chronic inflammatory responses, to skew the inflammatory cells to differentiate into immature phenotypes, as well as to increase T cell tolerance and dysfunction.⁵

As a highly mutated cancer, CRC progressively loses its tumor antigen and MHC-1 contents until immune escape prevails.⁶ Obesity tends to aid immune escape by conferring T cell populations with exhausted phenotypes.⁷ Exhausted T cells are a discrete T cell subset characterized by progressive loss of effector cytokines and impaired cytotoxicity.⁸ Actually, Tex represent a hyporesponsive state that stems from adaptation to persistent antigen and chronic T cell receptor stimulation.⁹

Recently, it has been elegantly demonstrated that HFD-induced obesity dampens the CD8⁺ TILs percentage and hampers their cytotoxicity.¹⁰ In another study, obesity was reported to induce immune aging and promote tumor growth across multiple strains and tumor types.¹¹ Obesity results in T cell exhaustion by increasing PD-1 expression and reducing IFN- γ and TNF- α production in TILs. Surprisingly, obesity augments the efficacy of the PD-1/PD-L1

blockade in various cancer patients and multiple tumor-bearing mice, suggest a controversial impact of obesity on cancers.¹¹

Dahuang Fuzi Baijiang decoction is a combined classical prescription from the “Synopsis of Prescriptions of the Golden Chamber,” which has been praised as the ancestor of traditional Chinese medical formulary. Hypothesizing that combination of Dahuang Fuzi decoction and Yiyi Fuzi Baijiang powder ameliorates obesity-induced T cell dysfunction, we tested this idea with a series of in vivo experiments in tumor-bearing mice. Our results show that DFB expands progenitor Tex counts and maintains appropriate adaptive T cell responses in both transgenic and diet-induced obese mice. These original findings would infuse novel meaning to the classical inheritance of traditional prescription and advance its clinical translation for tumor therapy.

2 | MATERIALS AND METHODS

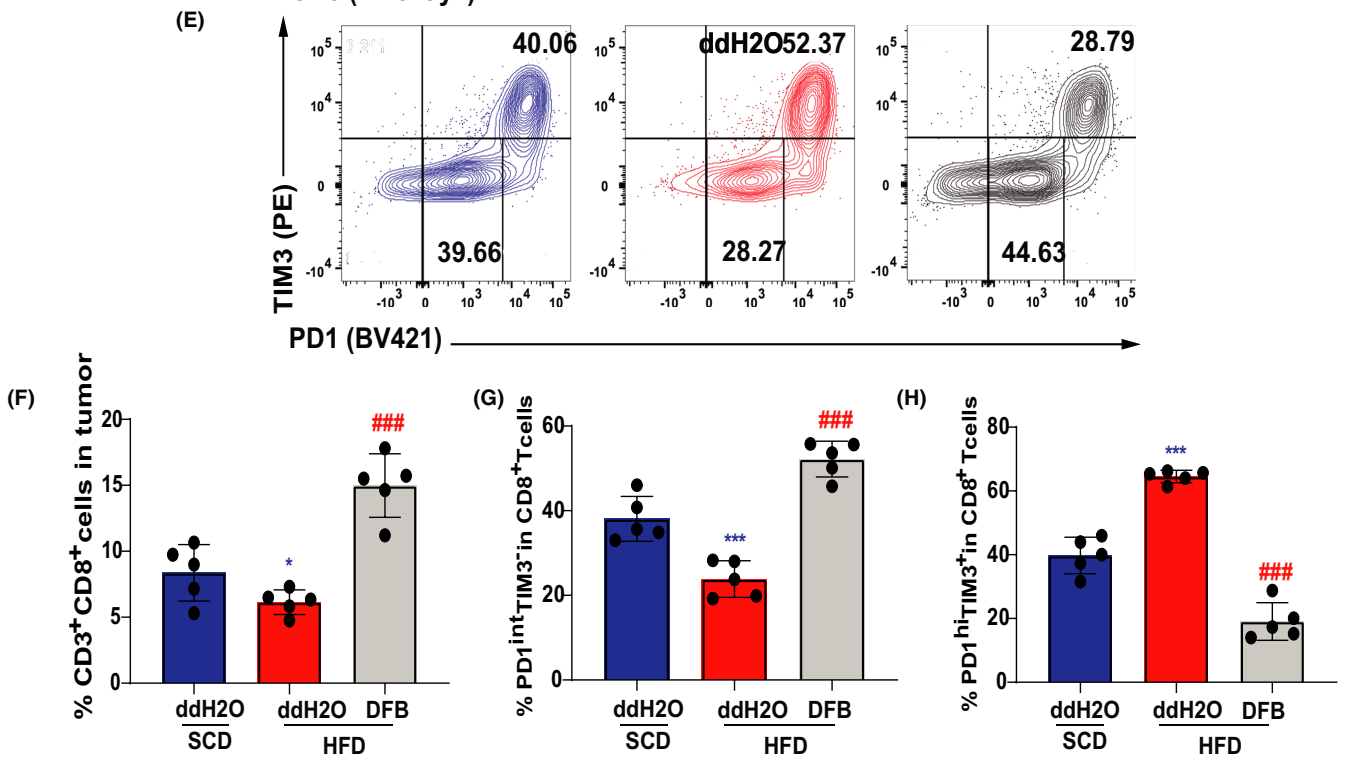
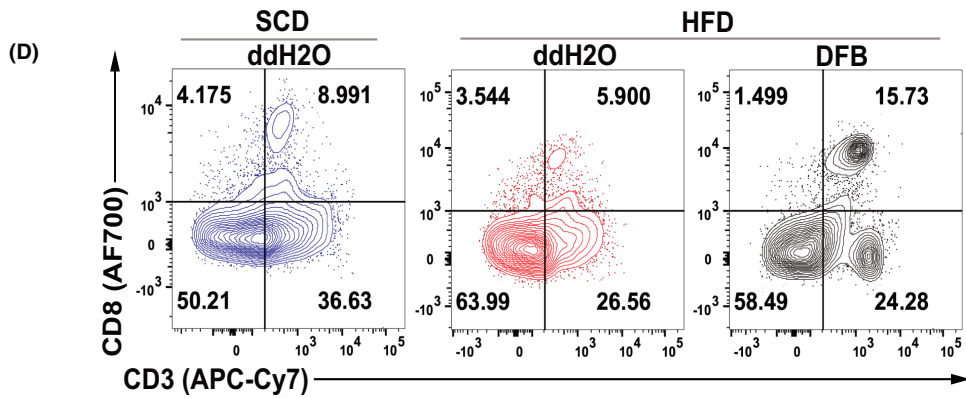
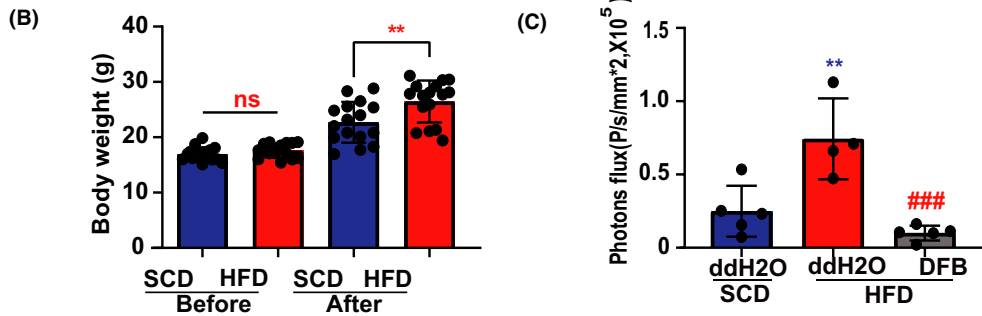
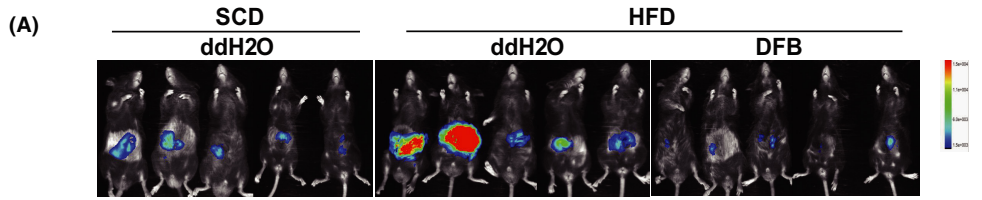
2.1 | Cell lines

MC38 cell line (Heyuan Biotech) stably expressing luciferase (MC38-luc, generated by stable transduction with RediFect Red-Fluc lentivirus from Perkin Elmer per manufacturer recommendations; Figure S1). Cells were cultured in normal DMEM without pyruvate supplemented with 10% FBS and 1% penicillin/streptomycin. Cells were cultured at 37°C in a humidified 5% CO₂ incubator.

2.2 | Mice

Eight-week-old C57BL/6, C57BL/KS-ob male mice were purchased from GemPharmatech Co., Ltd. For all experiments, 8-week-old mice were assigned to a normal diet. All mouse colonies and experimental animals were maintained in the same animal facility at Southern

FIGURE 1 Dahuang Fuzi Baijiang decoction (DFB) suppresses rapid growth of colorectal cancer in diet-induced obese (DIO) mice by restricting terminal exhausted T cells. (A) In vivo imaging of small animals in the colorectal orthotopic model. (B) Body weights of 8- to 16-week-old male control and DIO mice ($n = 5$ per group). (C) Fluorescence statistics of (A). (D) Representative flow plots and frequency of CD3⁺ CD8⁺ in tumor infiltration of mice in each group (top panel). Representative flow plots and frequency of PD-1 and TIM3 in tumor infiltration of mice in each group (bottom panel). (E) Statistical chart of the expression of CD3⁺ CD8⁺ in tumor infiltration each group of mice ($n = 5$ per group). (F) Statistical chart of the expression of PD-1^{mid}TIM3⁻ and PD-1^{hi}TIM3⁺ on the tumor-infiltrating CD8⁺ T cells of each group of mice ($n = 5$ per group). * $P < .05$, ** $P < .01$, *** $P < .001$ compared with standard chow diet (SCD) (ddH₂O) group. # $P < .05$, ## $P < .01$, ### $P < .001$ compared with the high-fat diet (HFD) (ddH₂O) group. Data in this figure are depicted as mean \pm SEM, with all individual points shown. Ordinary one-way ANOVA P values are shown. ns, not significant



Hospital of Southern Medical University and housed in specific pathogen-free conditions. All animals were used in accordance with animal care guidelines from the Southern Hospital Standing Committee on Animals and the National Institutes of Health. All mouse protocols were approved by the Southern Hospital Medical Area Standing Committee on Animals.

2.3 | Mouse tumor models

Orthotopic tumor transplantation was carried out as described previously.^{12,13} Briefly, tumor tissue was prepared by injecting MC38-luc cells into the abdominal flank of mice. The tumor slices were transplanted into the ileocecal area of the mice in situ. Mice were killed at humane end-points or day 10-14 for tissue harvest. Animals were kept in a sterile environment and treatment with DFB (intra-gastric administration) from day 3 after surgery, daily, or α PD-1 (i.p.), CCR2-RA-[R] (i.p.) every 2 days from day 5 after surgery. Weight was measured every 2 days. The mice were killed at the end of the experiments. Tumor, serum, liver, and spleen were collected for further experiments.

2.4 | Drug preparation

Dahuang Fuzi Baijiang decoction is comprised of five commonly used herbs (Table S1): Radix et Rhizoma Rhei (root or rhizome of perennial herbaceous plant *Rheum palmatum* L.), Radix Aconiti Lateralis Praeparata (root of perennial herbaceous plant *Aconitum carmichaelii* Debeaux), Herba Asari (root of *Asarum sieboldii* Miq.), Semen Coicis (nut of *Coix lacryma-jobi* L. var. *ma-yuen* Stapf), Herba Patriniae (entire plants of *Patrinia scabiosifolia* Fisch. ex Link. and *Patrinia villosa* Juss). The formula and amount of the prescription are listed in Table S1.

The raw herbs for DFB were purchased from Beijing Tongrentang Co. Ltd. The voucher specimens were deposited in the storage cabinet of Chinese traditional medicine at the School of Traditional Chinese Medicine, Southern Medical University. A voucher specimen was deposited in the herbarium of the School of Traditional Chinese Medicine. These were mixed in the ratio of 12:6:30:15:3 (dry weight). Aqueous extracts of DFB were extracted at 80°C by stirring it for 1 hour using 10 volumes of distilled water (v/m). Then we centrifuged the extract at 1500 g at room temperature. To obtain the semisolid DFB solution, the supernatant was collected and subjected to condensation under reduced pressure of 70°C. The DFB extracts were quality controlled by HPLC analysis with five

ingredients (Figures S2 and S3, Table S2). This was undertaken on a Shimadzu LC-20A HPLC system using a C18 column (Shimadzu VP ODS; 250 × 4.6 mm; particle size 5 μ m). The mobile phases comprised eluent A (water) and eluent B (methanol). The gradient flow was as follows: 0.00-125.00 minutes, 20%-90% B. The analysis was carried out at a flow rate of 1.0 mL/minute with photo-diode array detection at 254 nm. The injection volume was 20 μ L. Rhein (PubChem CID: 10168), fuziline (PubChem CID: 14163819), asarinin (PubChem CID: 11869417), coixol (PubChem CID: 10772), and quercetin (PubChem CID: 5280343) in the DFB sample were determined to be the five active compounds in Radix et Rhizoma Rhei, Radix Aconiti Lateralis Praeparata, Herba Asari, Semen Coicis and Herba Patriniae, respectively.

The α PD-1 (in vivo mAb anti-mouse PD-1) was purchased from BioX Cell and dissolved in PBS (200 μ g/kg/2 d). The CCR2 inhibitor CCR2-RA-[R] was purchased from MedChemExpress and dissolved in solvent (10% DMSO + 90% corn oil; 5 mg/kg/2 d). The HFD composition is listed in Table S3. The major reagents are listed in Tables S4-S7.

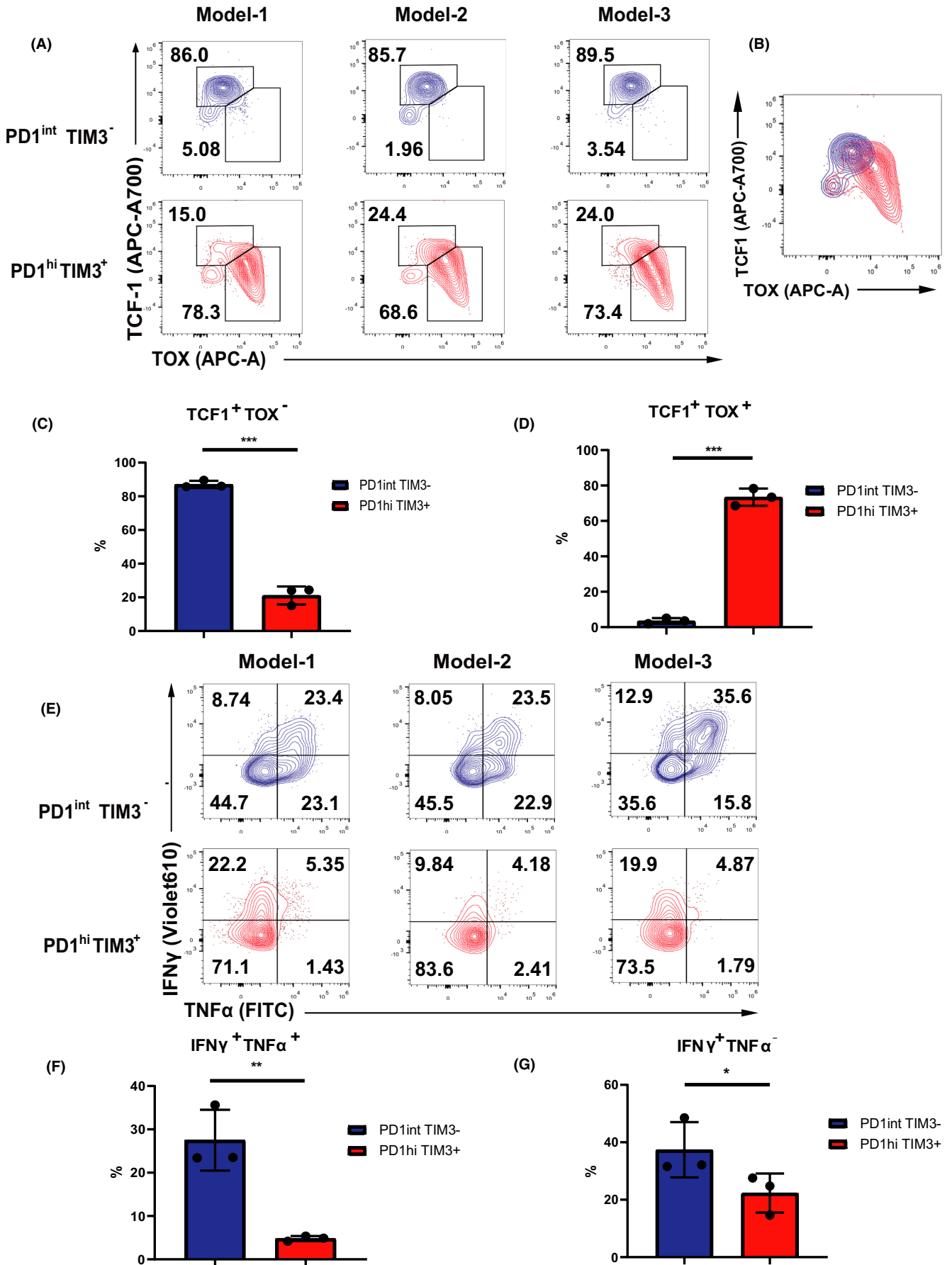
2.5 | Tumor-infiltrating leukocyte isolation

Tumor tissue (250 mg) was weighed, thoroughly cleaned, and gently cut it into small pieces. The chopped tissue was transferred to a 15-mL centrifuge tube and 1 mL PBS was added (protease inhibitor 1 mM PMSF, 0.01 mg/mL leupeptin, and 0.01 mg/mL aprotinin). The centrifuge tube was gently shaken (100 g at 4°C) and centrifuged for 1 minute, then the supernatant was aspirated (mainly damaged tissue and cell debris) with a Pasteur pipette. One milliliter of PBS was added to the precipitation sample and incubated in a 37°C, 5% CO₂ incubator for 1 hour. After incubation, the sample was centrifuged at 1000 g at 4°C for 3 minutes, the supernatant was removed, and the precipitate discarded. The sample was then centrifuged at 2000 g for 8 minutes at 4°C; the supernatant was removed and the precipitate discarded. Finally, the sample was centrifuged at 20,000 g at 4°C for 30 minutes; the supernatant was removed and the precipitate discarded.

2.6 | Enzyme-linked immunosorbent assay

Levels of TGF- β 1, IL-6, and CCL2 in TILs and serum were measured by ELISA (Table S6) following the manufacturer's instructions. We used a microplate reader (Multiskan; Thermo Fisher Scientific) to measure the absorbance at 450 nm.

FIGURE 2 TOX and TCF1 control T_{ex} differentiation status. (A) Representative flow plots of TOX and TCF1 ratio in PD1^{int} TIM3⁻ and PD1^{hi} TIM3⁺ cells ($n=3$ per group). (B) The overlap of TOX and TCF1 expression in TCF1⁺PD-1^{int} subset. (C, D) Statistical chart of A ($n=3$ per group). (E) Representative flow plots and frequency of IFN γ and TNF α expression among CD8⁺ TILs after Stimulation 6h with CD3/CD28 Ab in PD1^{int} TIM3⁻ and PD1^{hi} TIM3⁺ cells ($n=3$ per group). (F-G) Statistical chart of E ($n=3$ per group). Statistical significance was assessed by Student's t test (C-D; F-G). (not significant [ns], $p > 0.05$, * $p < 0.05$, ** $p < 0.01$)



2.7 | Flow cytometry

Primary mouse cells isolated from tumor were stained with fluorescent Abs and analyzed by flow cytometry. Briefly, the tissue samples were first mechanically dissociated using a scalpel, then enzymatically dissociated in digestion medium (2 mg/mL Collagenase I [Sigma] and 0.2 mg/mL DNase I [Sigma] in DMEM [Gibco]), and incubated for 30 minutes at 37°C with gentle rocking. Red blood cells were removed from the cell suspension using red blood cell lysis buffer (Beyotime), and the cells were filtered using a 70- μ m Flowmi tip strainer (VWR). Subsequent surface marker staining was undertaken in MACS buffer containing 1 \times PBS supplemented with 1% FBS and 2 mM EDTA. Intracellular staining for flow panels containing nuclear proteins was carried out using TCF1 (R&D Systems) and TOX (Miltenyi Biotech) transcription factor staining buffer set. For intracellular staining of cytoplasmic proteins, such as cytokines, the Fixation/Permeabilization Solution Kit (BD Biosciences) was used. Intracellular cytokine staining was carried out after 6 hours of stimulation with PMA (100 ng/mL) and ionomycin (500 ng/mL) in the presence of Golgi Stop at 37°C. Please see Table S7 for the fluorescently labeled Abs used for staining.

2.8 | Antibodies targeting surface or intracellular proteins

Intracellular cytokine staining was undertaken after 5 hours of ex vivo stimulation with GP33-41 peptide in the presence of Golgi Plug, Golgi Stop, and anti-CD107a. After stimulation, cells were stained with surface Abs, followed by fixation with Fixation/Permeabilization Buffer and then stained with intracellular Abs for TNF- α and IFN- γ using Permeabilization Wash Buffer according to the manufacturer's instructions. Data collection was carried out on a BD FACSymphony and analyzed using FlowJo version 10.4.1.

2.9 | Statistical analysis

Statistical analyses were undertaken using Graphpad Prism 8.0.2 (GraphPad Software). All assays were repeated at least three times and data are presented as the mean \pm SD. Differences between

groups were calculated utilizing ANOVA or a Student's *t* test for continuous variables. *P* < .05 was considered statistically significant.

3 | RESULTS

3.1 | Dahuang Fuzi Baijiang decoction suppresses rapid growth of CRC in DIO mice by restricting terminal Tex

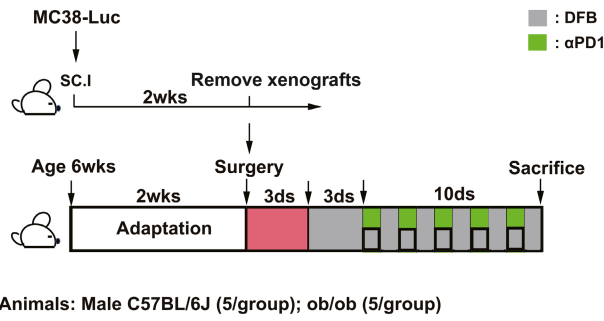
To explore the suitable dosage of well quality-controlled DFB extracts, the size of murine colon adenocarcinoma (MC38-luc; Figure S1) xenografts was recorded every other day (Figure S4A-C). Both middle dosage and high dosage significantly restricted tumor growth, whereas the middle dosage showed better performance in regressing growth kinetics (Figure S4D,E). Hence, DFB middle dosage was chosen for subsequent research because of the best curative efficacy among the three different doses.

High-fat diet-fed obese mice closely mimic the natural development of human obesity. We then monitored tumor growth in DIO mice (60% fat diet) vs control diet mice (control, standard chow diet). MC38 adenocarcinoma grew significantly faster in DIO mice, which showed an obvious increase of body weight compared with control counterparts (Figure 1A,B). Dahuang Fuzi Baijiang decoction enormously limited the growth of MC38 tumors, as indicated by luciferase-based bioluminescence imaging (Figure 1C), suggested that DFB is highly effective in suppressing tumor growth even under a protumoral obese microenvironment.

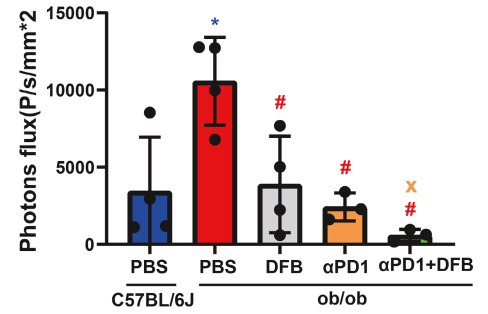
We next studied the function of DFB on T cell phenotype in the obese microenvironment (Figure S5A,B). Obesity slightly reduced the ratio of CD8⁺ TILs in the tumor bed, whereas DFB significantly increased the recruitment of CD8⁺ TILs (Figure 1D,F). Specifically, HFD resulted in a markedly higher frequency of PD-1^{hi}Tim3⁺ CD8⁺ TILs concomitant with an obvious decrease of the PD-1^{int}Tim3⁻ subset compared to control mice (Figure 1E,G,H). The PD-1^{hi}Tim3⁺ subset is generally defined as terminally differentiated exhausted T cells, whereas intermediate expression of PD-1 (PD-1^{int}) and coexistence of TCF-1 confer Tex with stem cell-like properties.^{9,14} Dahuang Fuzi Baijiang decoction increased the PD-1^{int} subset and lowered the number of PD-1^{hi}Tim3⁺ cells in the tumor. Taken together, DFB suppresses HFD-accelerated tumor progression by reserving the PD-1^{int} subset and decreasing Tex counts.

FIGURE 3 Dahuang Fuzi Baijiang decoction (DFB) reserves progenitor terminal exhausted T cells (Tex) to elicit immune response to anti-programmed cell death-1 (α PD-1). (A) Schema depicting experimental setup. (B) Body weights of WT C57BL/6J and *ob/ob* mice during the experiment. (C) In vivo imaging of small animals in the colorectal orthotopic model. (D) Representative flow plots and frequency of CD3⁺ CD8⁺ in tumor infiltration of mice in each group (top panel); Representative flow plots and frequency of PD-1 and TIM3 in tumor infiltration of mice in each group (top panel). Representative flow plots and frequency of PD-1 and TIM3 in tumor infiltration of mice in each group (bottom panel). (E) Statistical chart of the expression of CD3⁺ CD8⁺ in tumor infiltration each group of mice (*n* = 5 per group); (F) Statistical chart of the expression of tTex and pTex on the tumor-infiltrating CD8⁺ T cells of each group of mice (*n* = 5 per group). **P* < .05; ***P* < .01; ****P* < .001, compared with C57BL/6J (PBS) group. #*P* < .05; ##*P* < .01; ###*P* < .001, compared with *ob/ob* (PBS) group. **p* < .05, compared with *ob/ob* (α PD1 + DFB) group. Data in this figure are depicted as mean \pm SEM, with all individual points shown. Ordinary one-way ANOVA *P* values are shown

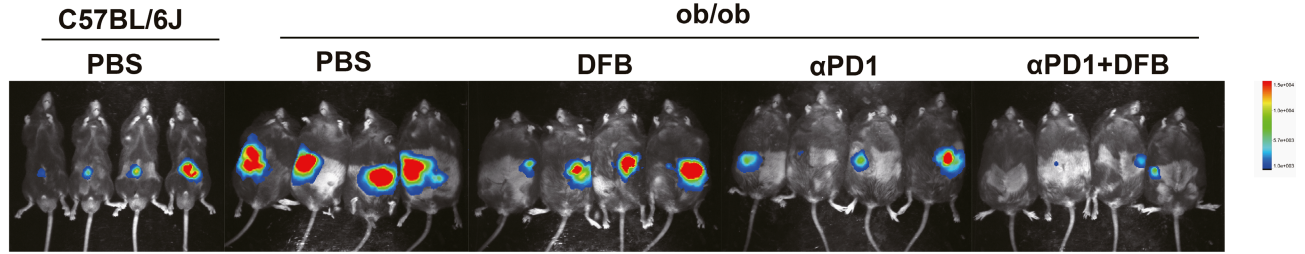
(A)



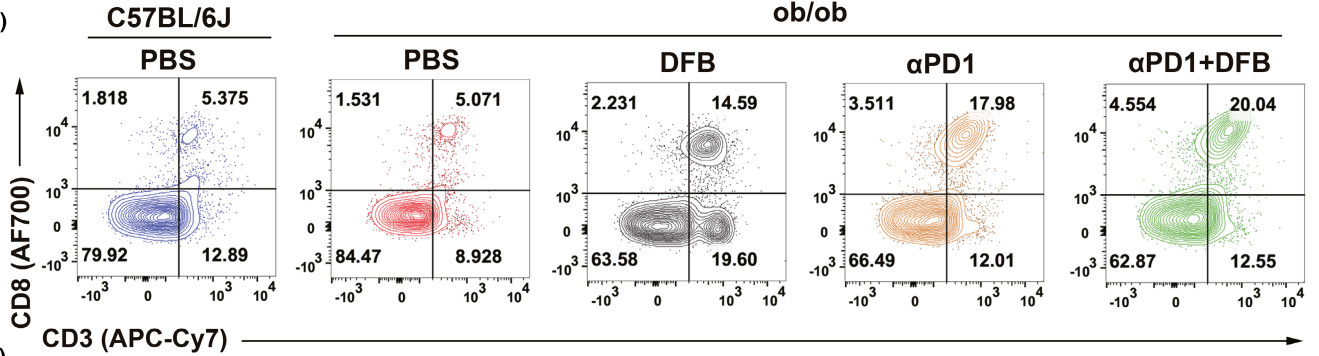
(B)



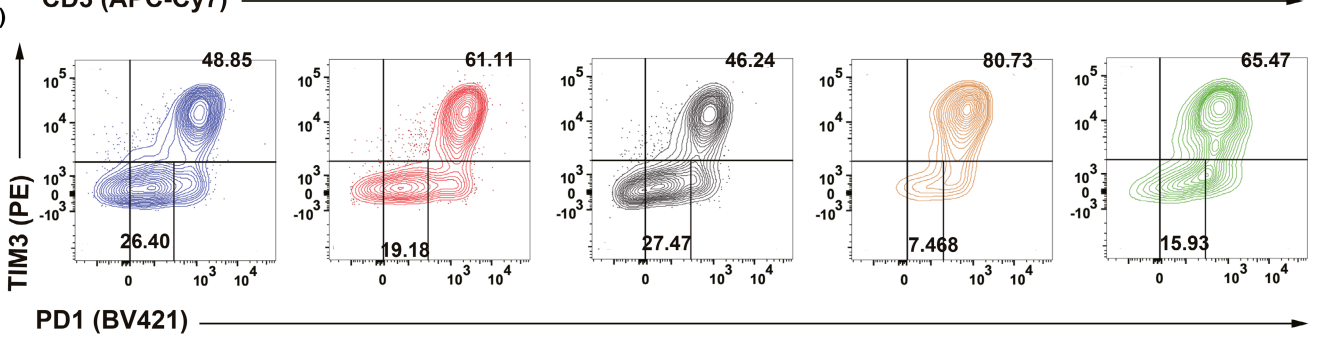
(C)



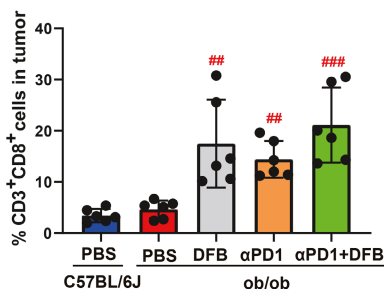
(D)



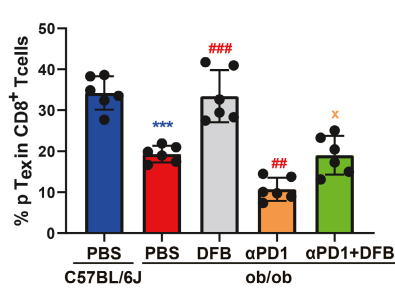
(E)



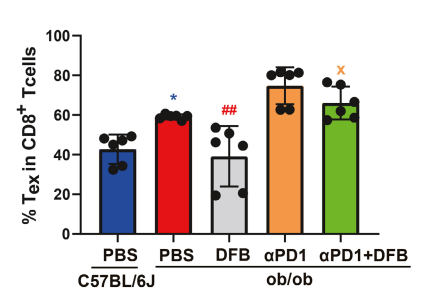
(F)



(G)



(H)



3.2 | TOX and TCF1 control Tex differentiation status

Terminally differentiated Tex is the driving force to form immunosuppressive microenvironment, whereas progenitor Tex subset is critical for generating response to PD-1 blockade.¹⁵⁻¹⁷ To characterize the differentiation state of the two subsets, we sorted and analyzed transcription activity of TCF1 and thymocyte selection-associated high mobility group box (TOX) (Figure S6C). PD-1^{int}TIM3⁺ cells are characterized by strong expression of TCF1 which is absent in PD-1^{hi}Tim3⁺ cells (Figure 2A, C). These TCF1⁺PD-1^{int} progenitor cells can expand and yield terminal exhausted PD-1^{hi}Tim3⁺ cells. We observed a highly expression of TOX in the PD-1^{hi}Tim3⁺ subset

(Figure 2A, D). TOX transcriptionally activates co-inhibitory receptor gene *Pdcd1* and stimulates the transcription of *Tcf7* which is the encoding gene for TCF1. We also noticed an overlap of TOX and TCF1 expression in TCF1⁺PD-1^{int} subset (Figure 2B), suggested that TOX may act upstream of TCF1 to drive the differentiation from progenitor to terminal Tex.

As Tex progressively lose its effector function in a hierarchical pattern, we examined the alterations of effector cytokines with an *ex vivo* experiment. The sorted TCF1⁺PD-1^{int} and PD-1^{hi}Tim3⁺ cells were stimulated with CD3 and CD28 antibody (Figure S6C). TCF1⁺PD-1^{int} cells displayed robust ability to produce TNF α and IFN γ . However, PD-1^{hi}Tim3⁺ exhibited defects in generating IFN- γ while showed residue competence to produce TNF α (Figure 2E-F). Loss of IFN γ has been

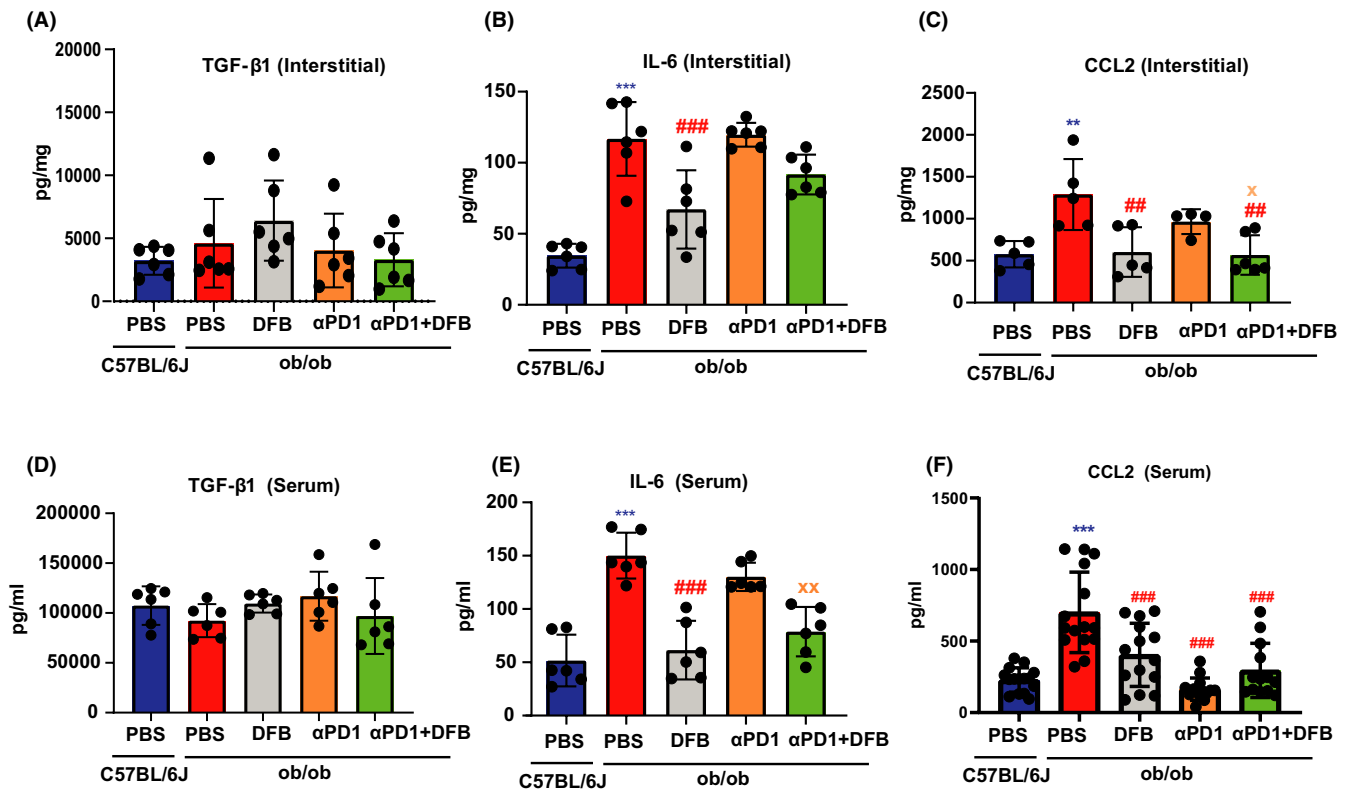
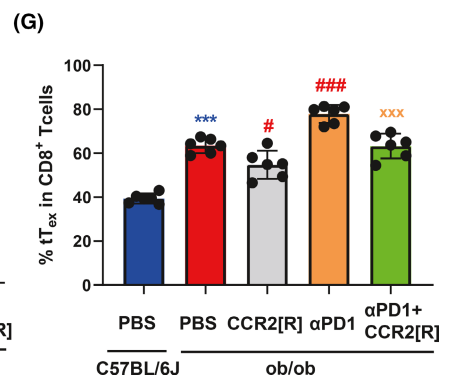
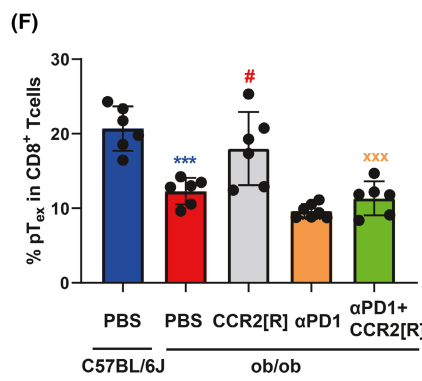
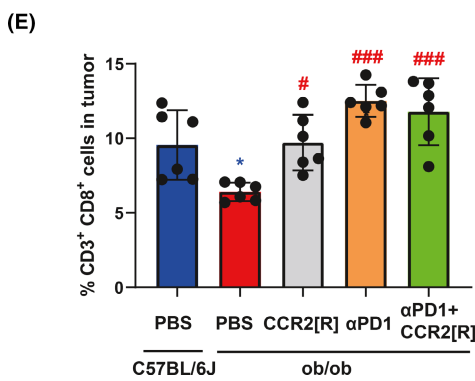
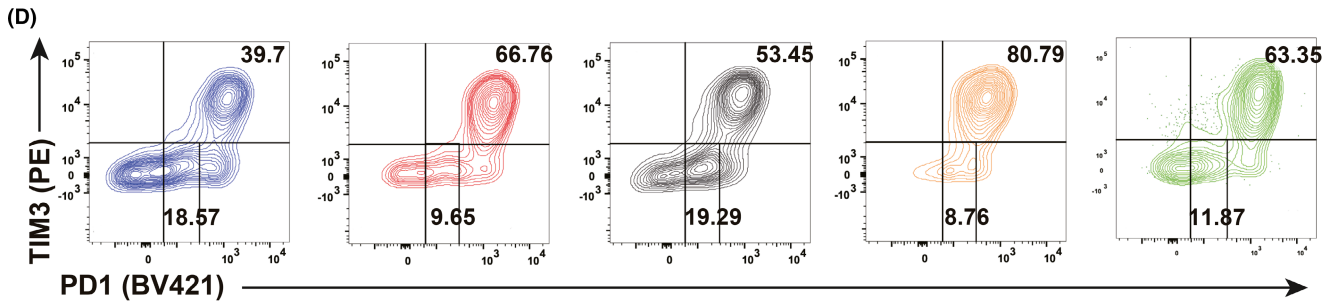
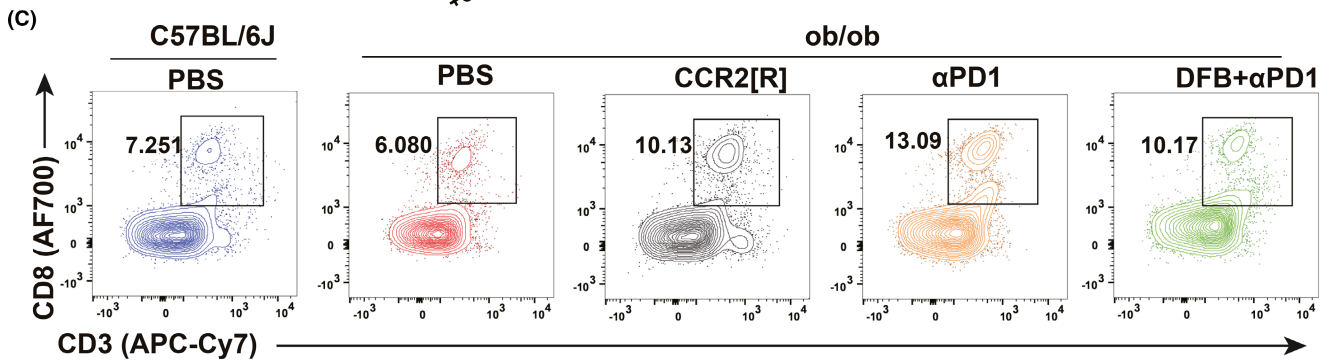
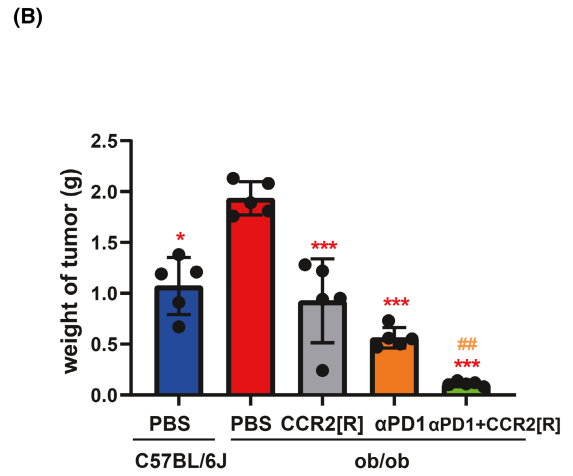
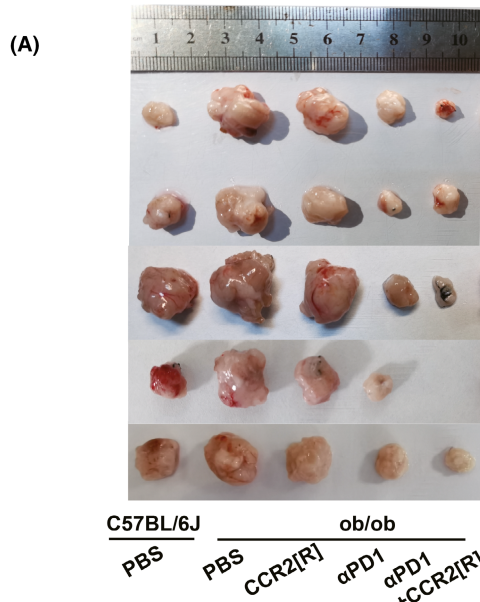


FIGURE 4 Dahuang Fuzi Baijiang decoction (DFB) reduces tumor interstitial and serum chemokine (C-C motif) ligand 2 (CCL2) production. Contents of key adipokines in tumor interstitial fluid and serum. Transforming growth factor- β 1 (TGF- β 1) in tumor interstitial fluid (A) and serum (D). Interleukin-6 (IL-6) in tumor interstitial fluid (B) and serum (E). CCL2 in tumor interstitial fluid (C) and serum (F). * $P < .05$, ** $P < .01$, *** $P < .001$, compared with *ob/ob* (PBS) group. # $P < .05$, ## $P < .01$, ### $P < .001$, compared with *ob/ob* (anti-programmed cell death-1 [α PD-1] + DFB) group. Data in this figure are depicted as mean \pm SEM, with all individual points shown. Ordinary one-way ANOVA P values are shown

FIGURE 5 CCR2 inhibitor suppresses the shift from pTex to tTex. (A) Tumor weight of MC38 subcutaneously inoculated in 8-week-old C57BL/6J ($n = 5$) and *ob/ob* ($n = 5$) male mice. Tumor weight depicted as mean \pm SEM. (B) Statistical chart of the tumor weight in each group ($n = 5$ per group). (C) Representative flow plots of CD3⁺ CD8⁺ ratio in tumor-bearing mice in each group (Above); Representative flow plots of PD1 and TIM3 ratio in tumor-bearing mice in each group (Below). (D) Statistical chart of the ratio of CD3⁺ CD8⁺ in tumor infiltration each group ($n = 5$ per group). (E) Statistical chart of the ratio of terminal exhausted T cells (tTex) and progenitor exhausted T cells (pTex) in the tumor-infiltrating CD8⁺ T cells of each group ($n = 5$ per group). (F) Statistical chart of the ratio of tTex and pTex in the tumor-infiltrating CD8⁺ T cells of each group ($n = 5$ per group). Compared with C57BL/6J (PBS) group, * $p < 0.05$; ** $p < 0.01$; *** $p < 0.001$. Compared with *ob/ob* (PBS) group, # $p < 0.05$; ## $p < 0.01$; ### $p < 0.001$. Compared with *ob/ob* (α PD1+CCR2-RA-[R]) group, ** $p < 0.01$. Data in this figure are all depicted as mean \pm SEM, with all individual points shown. Ordinary one-way ANOVA p values are shown



considered occurring at the late stage of exhaustion¹⁴, our results suggested that the cytotoxicity defect in PD-1^{hi}Tim3⁺ cells is corresponding to the terminally exhausted state (Figure 2E, G). These distinct

fingerprints of Tex suggested that TOX and TCF1 drive the evolution between progenitor and terminal Tex which determine the exhausted status and their response to checkpoint blockade.

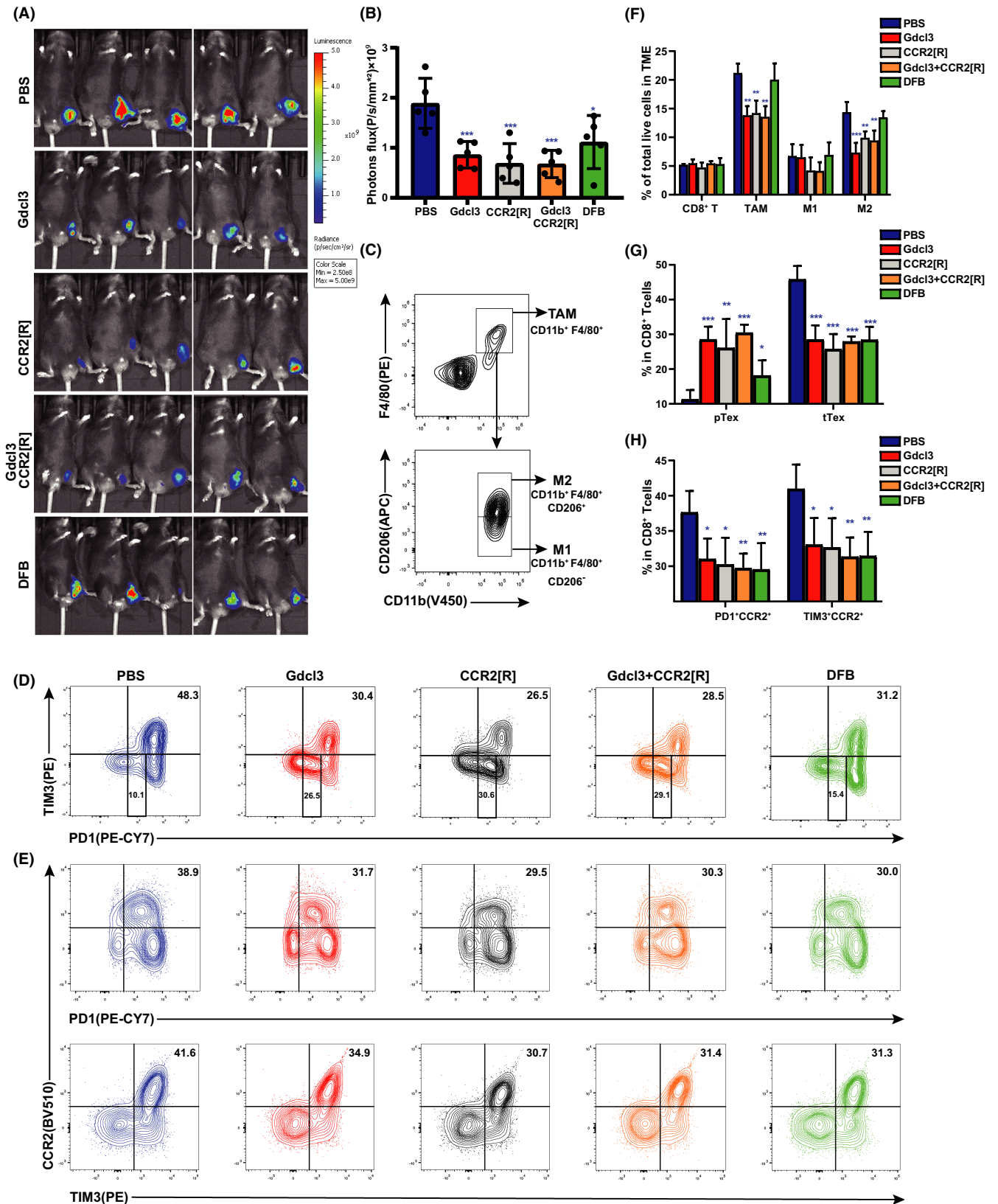


FIGURE 6 Dahuang Fuzi Baijiang decoction (DFB) inhibits shift from progenitor exhausted T cells (pTex) to terminal exhausted T cells (tTex) independent of macrophages. (A) In vivo imaging of small animals in the colorectal subcutaneous model. (B) Fluorescence statistics of figure (A). (C) Flow cytometry gating strategies used to define tumor-associated macrophages (TAM) (CD11b⁺F4/80⁺), M1-TAM (CD11b⁺F4/80⁺CD206⁻) and M2-TAM (CD11b⁺F4/80⁺CD206⁺). (D) Representative flow plots and frequency of PD-1 and TIM3 in tumor infiltration of mice in each group. (E) Representative flow plots and frequency of recombinant chemokine C-C-motif receptor 2 (CCR2) on the tumor-infiltrating CD8⁺ Tex cells of each group. (F) Relative percentages of the tumor-infiltrating inflammatory cells, as determined by FACS, in the tumor tissues of mice subjected to various treatments. These include CD8⁺ tumor-infiltrating lymphocytes, TAM, M1-TAM, and M2-TAM ($n = 5$ per group). (G) Statistical chart of the expression of tTex and pTex on the tumor-infiltrating CD8⁺ T cells of each group of mice ($n = 5$ per group). (H) Statistical chart of the expression of CCR2 on the tumor-infiltrating CD8⁺ Tex cells of each group of mice ($n = 5$ per group). * $P < .05$, ** $P < .01$, *** $P < .001$, compared with C57BL/6J (PBS) group. Data in this figure are depicted as mean \pm SEM, with all individual points shown. Ordinary one-way ANOVA P values are shown. GdCl₃, gadolinium chloride

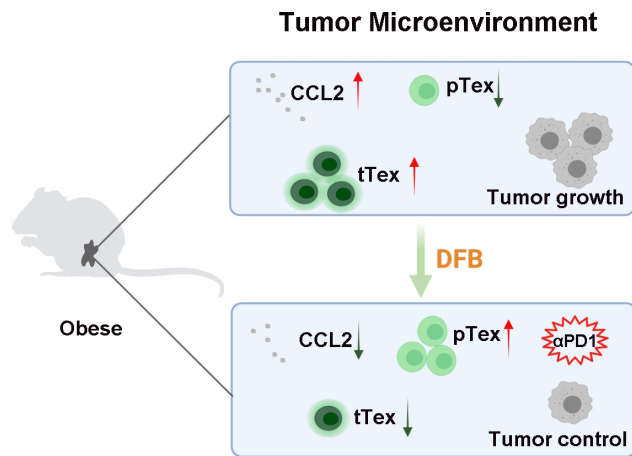


FIGURE 7 Summary illustration of the effect of Dahuang Fuzi Baijiang decoction (DFB) on colorectal cancer tumor growth in obese mice. α PD-1, anti-programmed cell death-1; CCL2, chemokine (C-C motif) ligand 2; pTex, progenitor exhausted T cells; tTex, terminal exhausted T cells

3.3 | Dahuang Fuzi Baijiang decoction reserves progenitor Tex to elicit immune response to α PD-1

As PD-1^{int}TCF-1⁺ progenitor TILs are poised to respond to PD-1 blockade, we reasoned that DFB might coordinate α PD-1 response by modulating PD-1 expression in CD8⁺ T cells. *Ob/ob* mice carry a spontaneous mutation at the leptin locus that leads to obesity, hyperglycemia, and elevated plasma insulin. *Ob/ob* mice were visibly obese with elevated body weight and abdominal circumference (Figure S6A,B). Mirroring the protumorigenic activity of DIO, the *ob/ob* phenotype drastically accelerated MC38 tumor growth compared to its corresponding C57BL/6J background (Figure S7). We established a subcutaneous ectopic transplanted tumor model in *ob/ob* mice (Figure 3A). Dahuang Fuzi Baijiang decoction not only moderately attenuated tumor growth (Figure 3B,C), but displayed prominent cooperative efficacy in limiting tumor size in *ob/ob* mice (Figure S1B,C).

To investigate whether reduced growth rates of tumors by DFB was due to control by T cells, we genotyped the T cells in the tumor with PD-1 and TIM3 (Figure S5A,B). Dahuang Fuzi Baijiang decoction augmented the number of CD8⁺ T cells and synergized the effects of α PD-1 (Figure 3D,F). As expected, *ob/ob* mice increased the percentage of PD-1^{hi}Tim3⁺ cells, corresponding to a reduction of

PD-1^{int} cells (Figure 3E,G,H). Dahuang Fuzi Baijiang decoction substantially decreased the ratio of terminal PD-1^{hi}Tim3⁺ Tex to ameliorate the immunosuppressive condition. It also increased the number of PD-1^{int} T cells that serve to respond to α PD-1 immunotherapy. Together, DFB curbs the tumor growth by limiting the PD-1^{hi}Tim3⁺ subset and amplifying PD-1^{int} population to enhance the efficacy of PD-1 checkpoint blockade.

3.4 | Dahuang Fuzi Baijiang decoction reduces tumor interstitial and serum CCL2 production

Obesity has been demonstrated to induce a chronic, low-grade inflammatory status with increased adipokines, such as IL-6, TGF- β , leptin, and TNF- α , as well as elevated levels of CCL2. *Ob/ob* genotype elevated IL-6 in tumor interstitial fluid, but had no obvious impact on TGF- β secretion compared to age-matched WT mice (Figure 4A,D). Dahuang Fuzi Baijiang decoction substantially depressed tumor interstitial IL-6 content but displayed no synergistic effects with α PD-1 on IL-6 levels (Figure 4B,E).

Chemokine (C-C motif) ligand 2, which is symbolically presented at high levels in obesity, gives rise to immune evasion through PD-1 signaling.¹⁸ We first assessed the effects of DFB on CCL2 in *ob/ob* mice. Dahuang Fuzi Baijiang decoction reversed obesity-raised stromal CCL2 content. Although α PD-1 alone could not lower CCL2 secretion, DFB helped α PD-1 inhibitor to reduce stromal CCL2 levels (Figure 4C,F). We next evaluated the impact of DFB in DIO mice and observed a remarkably similar pattern. Dahuang Fuzi Baijiang decoction attenuated interstitial CCL2 content in HFD-feeding obese mice. Additionally, we also measured the alteration of serum CCL2 contents. As expected, either DFB or α PD-1, or the two together, decreased serum CCL2 elevation that is induced by the obese background. Collectively, DFB dampens obesity-driven tumor interstitial and serum CCL2 production both in DIO and transgenic obese mice.

3.5 | Recombinant chemokine C-C-motif receptor 2 inhibitor blocks shift from progenitor Tex to terminal Tex

As elevated CCL2 expression drives PD-1 inhibitor resistance¹⁹ and CCR2 antagonism enhances tumor response to α PD-1

monotherapy,²⁰ we then tested whether the CCL2-CCR2 axis contributes to Tex differentiation with a specific inhibitor, CCR2-RA-[R]. As we found earlier, MC38 tumor growth was accelerated in *ob/ob* mice compared with control C57BL6/J mice (Figure 5A,B). There was no significant change in the weight of the spleen or liver (Figure S8). The CCR2 inhibitor restrained tumor growth and increased CD8⁺ T cell infiltration (Figure 5C,E).

We also observed a reduction of progenitor PD-1^{int} number in *ob/ob* mice compared to their WT counterparts. Importantly, CCR2 inhibitor enhanced the percentage of progenitor PD-1^{int} cells, and also expanded this subset when combined with α PD-1 immunotherapy (Figure 5D,F,G). Corresponding to its protumor phenotype, *ob/ob* mice also increased the ratio of terminal PD-1^{hi}TIM3⁺ CD8⁺ TILs, whereas CCR2 inhibitor reduced the counts of this subset. Hence, obesity enhanced tumor interstitial CCL2 to facilitate the differentiation from progenitor to terminal Tex. Dahuang Fuzi Baijiang decoction exerts its antitumor activity through disturbing CCL2/CCR2-mediated terminal T cell exhaustion.²¹ Together, DFB decreases obesity-driven CCL2 secretion and reverses the Tex differentiation shift to regress CRC progression.

3.6 | Dahuang Fuzi Baijiang decoction inhibits terminal Tex differentiation by disrupting T cell CCR2 signaling

Apart from T cells, CCR2 is predominantly expressed by monocytes/macrophages.²² To elucidate the role of macrophages on CD8⁺ T cell differentiation, a monocyte/macrophage depleting agent, GdCl3, was used. GdCl3 restricts tumor growth in *ob/ob* mice, similar to the effects of CCR2 antagonist. Our results also show that combining GdCl3 and CCR2 antagonist does not result in an additive or synergistic effect in suppressing the growth of MC38 xenografted tumor (Figure 6A,B), which is consistent with a previous report.²³

Treatment with GdCl3 or/and CCR2 inhibitor significantly reduced the infiltration of tumor-associated macrophages (CD11b⁺ F4/80⁺), especially the proportion of M2 (CD11b⁺ F4/80⁺ CD206⁺; Figure 6C,F). CD8⁺ T cell genotyping shows that DFB, GdCl3, and/or CCR2 inhibitor restrains the differentiation from progenitor to terminal Tex (Figure 6D,G). However, DFB does not cause appreciable changes in macrophage subsets, suggested that progenitor-prone differentiation of CD8⁺ T cells caused by DFB is not dependent on macrophages. Further genotyping shows that the CCR2⁺CD8⁺ T cell subset is mainly composed of PD-1⁺TIM3⁺ cells, which is defined as terminal Tex (Figure 6E,H). Taken together, the CCR2⁺CD8⁺ subset is characterized as terminal Tex; DFB inhibits terminal Tex differentiation by disrupting the CCL2/CCR2 axis in T cells.

4 | DISCUSSION

Obesity boosts TILs entering an exhausted state. T cell exhaustion represents a compromise to continuous antigen stimulation, which allows T cells to control tumor growth without causing detrimental

immunological pathology. However, cancer cells have hijacked the exhaustion tactics during evolution, encouraging the adaptive immune system to “tolerate” them so as to gain the survival allowance. The “host-pathogen stalemate” during obesity reveals that the “energy”-like hyporesponsive state of T cell and chronic inflammation can be coupled.⁹ So, DFB might suppress obesity-associated incidence of CRC by ameliorating the adaptive state of T cell hyporesponsiveness and dampening low-grade inflammation.^{24,25}

Of particular note, DFB increases the infiltration of the PD-1^{int}TCF1⁺ subset, which can be ascribed to progenitor/stem-like exhausted T cells.²⁶ The specific pool of exhausted T cells retains partial protective capability once reinvigorated by blockade of the PD-1 pathway.^{27,28} Importantly, these progenitor cells hold potential to proliferate and to yield terminally differentiated Tex. Dahuang Fuzi Baijiang decoction inhibits the shift of progenitor exhausted T cells to terminally differentiated T cells and augments the effects of PD-1 checkpoint blockade. So, DFB provides synergistic therapeutic benefit with checkpoint blockade to enhance the enhancer in tumor immunity.²¹

The hyperplasia and hypertrophy of adipocytes in obesity trigger chronic inflammation by increasing the secretion of CCL2.²⁹ It has been well demonstrated that the CCL2/CCR2 axis enhances tumor progression by amplifying the recruitment of myeloid-derived suppressor cells and metastasis-promoting monocytes.^{22,30} Our results give additional evidence that CCL2 compels T cells to differentiate into a terminally exhausted phenotype which accelerates the progression of CRC.

Recombinant chemokine C-C-motif receptor 2 antagonism promotes tumor response to PD-1 inhibitor in multiple cancer types,^{19,31} indicating that the CCR2⁺CD8⁺ subset may be immunosuppressive. Dahuang Fuzi Baijiang decoction reverses CCL2 production in the obese microenvironment and holds Tex back into a progenitor state. So, targeting CCL2/CCR2 might be a suitable strategy in rescuing terminal T cell exhaustion.

Altogether, DFB dampens CCL2 and preserves progenitor Tex in the obese microenvironment to restrain CRC progression (Figure 7). Obesity enhances tumor progression by raising CCL2 secretion, which recruits terminally exhausted T cells to establish a healthy-Qi deficient microenvironment. Dahuang Fuzi Baijiang decoction strengthens healthy-Qi and eliminates cancerous lesions by restricting CCL2/CCR2-mediated recruitment of exhausted T cells. Dahuang Fuzi Baijiang decoction also inhibits the polarization of progenitor T cells to terminal exhausted T cells. The preservation of progenitor Tex is indispensable for the response to PD-1 checkpoint blockade.¹⁷ Taken together, our outcomes pave a novel avenue to use classic prescriptions to cure cancerous disease through regulating adaptive immunology. Although the two constituent formulae of DFB have been used for thousands of years, the immunomodulatory properties of DFB still need further confirmation from clinical practice.

ACKNOWLEDGMENTS

This work was supported by the National Science Foundation of China (81974554, 81774172, 81904075), Key-Area Research and

Development Program of Guangdong Province, Modernization of Chinese Medicine in Lingnan (2020B1111100011), Planned Science Technology Project of Guangzhou (202002030111).

CONFLICT OF INTEREST

The authors declare that they have no competing interests.

ORCID

Xuegang Sun  <https://orcid.org/0000-0001-6581-0520>

REFERENCES

- Steele CB, Thomas CC, Henley SJ, et al. Vital Signs: trends in incidence of cancers associated with overweight and obesity - United States, 2005-2014. *MMWR Morb Mortal Wkly Rep.* 2017;66:1052-1058.
- Eheman C, Henley SJ, Ballard-Barbash R, et al. Annual report to the nation on the status of cancer, 1975-2008, featuring cancers associated with excess weight and lack of sufficient physical activity. *Cancer-Am Cancer Soc.* 2012;118:2338-2366.
- Calle EE, Kaaks R. Overweight, obesity and cancer: epidemiological evidence and proposed mechanisms. *Nat Rev Cancer.* 2004;4:579-591.
- Bardou M, Barkun AN, Martel M. Obesity and colorectal cancer. *Gut.* 2013;62:933-947.
- Kanneganti TD, Dixit VD. Immunological complications of obesity. *Nat Immunol.* 2012;13:707-712.
- Woodall MJ, Neumann S, Campbell K, Pattison ST, Young SL. The effects of obesity on anti-cancer immunity and cancer immunotherapy. *Cancers (Basel).* 2020;12:1230.
- Xie Q, Ding J, Chen Y. Role of CD8(+) T lymphocyte cells: interplay with stromal cells in tumor microenvironment. *Acta Pharm Sin B.* 2021;11:1365-1378.
- Yang Y, Liu F, Liu W, et al. Analysis of single-cell RNAseq identifies transitional states of T cells associated with hepatocellular carcinoma. *Clin Transl Med.* 2020;10:e133.
- Blank CU, Haining WN, Held W, et al. Defining 'T cell exhaustion'. *Nat Rev Immunol.* 2019;19:665-674.
- Ringel AE, Drijvers JM, Baker GJ, et al. Obesity shapes metabolism in the tumor microenvironment to suppress anti-tumor immunity. *Cell.* 2020;183:1848-1866.
- Wang Z, Aguilar EG, Luna JI, et al. Paradoxical effects of obesity on T cell function during tumor progression and PD-1 checkpoint blockade. *Nat Med.* 2019;25:141-151.
- Zhao L, Wang H, Liu C, et al. Promotion of colorectal cancer growth and metastasis by the LIM and SH3 domain protein 1. *Gut.* 2010;59:1226-1235.
- Han Q, Xu L, Lin W, et al. Long noncoding RNA CRCMSL suppresses tumor invasive and metastasis in colorectal carcinoma through nucleocytoplasmic shuttling of HMGB2. *Oncogene.* 2019;38:3019-3032.
- McLane LM, Abdel-Hakeem MS, Wherry EJ. CD8 T cell exhaustion during chronic viral infection and cancer. *Annu Rev Immunol.* 2019;37:457-495.
- Sakuishi K, Apetoh L, Sullivan JM, Blazar BR, Kuchroo VK, Anderson AC. Targeting Tim-3 and PD-1 pathways to reverse T cell exhaustion and restore anti-tumor immunity. *J Exp Med.* 2010;207:2187-2194.
- Dammeijer F, van Gulijk M, Mulder EE, et al. The PD-1/PD-L1-checkpoint restrains T cell immunity in tumor-draining lymph nodes. *Cancer Cell.* 2020;38:685-700.
- Miller BC, Sen DR, Al AR, et al. Subsets of exhausted CD8(+) T cells differentially mediate tumor control and respond to checkpoint blockade. *Nat Immunol.* 2019;20:326-336.
- Yang H, Zhang Q, Xu M, et al. CCL2-CCR2 axis recruits tumor associated macrophages to induce immune evasion through PD-1 signaling in esophageal carcinogenesis. *Mol Cancer.* 2020;19:41.
- Choi J, Lee HJ, Yoon S, et al. Blockade of CCL2 expression overcomes intrinsic PD-1/PD-L1 inhibitor-resistance in transglutaminase 2-induced PD-L1 positive triple negative breast cancer. *Am J Cancer Res.* 2020;10:2878-2894.
- Tu MM, Abdel-Hafiz HA, Jones RT, et al. Inhibition of the CCL2 receptor, CCR2, enhances tumor response to immune checkpoint therapy. *Commun Biol.* 2020;3:720.
- Gu Y, Liu Y, Cao X. Evolving strategies for tumor immunotherapy: enhancing the enhancer and suppressing the suppressor. *Natl Sci Rev.* 2015;4:161-163.
- Hartwig T, Montinaro A, von Karstedt S, et al. The TRAIL-induced cancer secretome promotes a tumor-supportive immune microenvironment via CCR2. *Mol Cell.* 2017;65:730-742.
- Li X, Yao W, Yuan Y, et al. Targeting of tumour-infiltrating macrophages via CCL2/CCR2 signalling as a therapeutic strategy against hepatocellular carcinoma. *Gut.* 2017;66:157-167.
- Sinicrope FA, Foster NR, Sargent DJ, O'Connell MJ, Rankin C. Obesity is an independent prognostic variable in colon cancer survivors. *Clin Cancer Res.* 2010;16:1884-1893.
- Chen X, Pan X, Zhang W, et al. Epigenetic strategies synergize with PD-L1/PD-1 targeted cancer immunotherapies to enhance antitumor responses. *Acta Pharm Sin B.* 2020;10:723-733.
- Chen Z, Ji Z, Ngiow SF, et al. TCF-1-centered transcriptional network drives an effector versus exhausted CD8 T cell-fate decision. *Immunity.* 2019;51:840-855.
- Pauken KE, Wherry EJ. SnapShot: T cell exhaustion. *Cell.* 2015;163:1038.
- Beltra JC, Manne S, Abdel-Hakeem MS, et al. Developmental relationships of four exhausted CD8(+) T Cell subsets reveals underlying transcriptional and epigenetic landscape control mechanisms. *Immunity.* 2020;52:825-841.
- Catalan V, Gomez-Ambrosi J, Rodriguez A, et al. IL-32alpha-induced inflammation constitutes a link between obesity and colon cancer. *Oncimmunology.* 2017;6:e1328338.
- Yang Y, Li L, Xu C, et al. Cross-talk between the gut microbiota and monocyte-like macrophages mediates an inflammatory response to promote colitis-associated tumorigenesis. *Gut.* 2021;70(8):1495-1506.
- Shi L, Wang J, Ding N, et al. Inflammation induced by incomplete radiofrequency ablation accelerates tumor progression and hinders PD-1 immunotherapy. *Nat Commun.* 2019;10:5421.

SUPPORTING INFORMATION

Additional supporting information may be found in the online version of the article at the publisher's website.

How to cite this article: Xu Y, Wang H, Wang T, et al. Dahuang Fuzi Baijiang decoction restricts progenitor to terminally exhausted T cell differentiation in colorectal cancer. *Cancer Sci.* 2022;113:1739-1751. doi:[10.1111/cas.15311](https://doi.org/10.1111/cas.15311)